Compositional variations in the near surface layers, an atomprobe study of cosegregation of sulfur in Pt–Rh and Pt–Ir alloys

M. Ahmad and T. T. Tsong

Citation: The Journal of Chemical Physics **83**, 388 (1985); doi: 10.1063/1.449782
View online: http://dx.doi.org/10.1063/1.449782
View Table of Contents: http://scitation.aip.org/content/aip/journal/jcp/83/1?ver=pdfcov
Published by the AIP Publishing

Compositional variations in the near surface layers, an atom-probe study of cosegregation of sulfur in Pt–Rh and Pt–Ir alloys

M. Ahmad and T. T. Tsong
Department of Physics, The Pennsylvania State University, University Park, Pennsylvania 16802

(Received 17 December 1984; accepted 29 March 1985)

Equilibrium composition depth profiles with true single atomic layer depth resolution have been obtained for the (001) plane of a Pt–Ir and five Pt–Rh alloys using the atom-probe field ion microscope. Pt segregates to the top two layers in Pt–Ir and Rh segregates to the top layer in Pt–Rh alloys after annealing at 700 °C for 5 min. In addition, an overlayer of sulfur is found to cosegregate to the surface of these alloys even though the bulk impurity content is less than 100 ppm. The coverage of sulfur overlayer for Pt–Rh alloys varies between 0.22 to 0.52 of a monolayer, and it increases with increasing surface Rh concentration. The depth dependence of the composition depth profiles has been found to be monotonic for the Pt–Ir alloy and nonmonotonic, or possibly oscillatory, for the Pt–Rh alloys. Pending the uncertainty of the effect of the sulfur overlayer, Pt segregation in Pt–Ir is consistent with most theoretical models, and Rh segregation in Pt–Rh is consistent with the bond-breaking model and the atomic model, but is inconsistent with a surface energy model and an electronic model. Rh segregation may also be an effect of chemisorption enhanced surface segregation. While the experimental result on the top surface layer can be explained by various theoretical models, the compositional variation in the near surface layers may shed some light on the atomic interactions in the surface region. For the Pt–Ir alloy, we have also observed a diffusion kinetic effect in a composition depth profile.

I. INTRODUCTION

It is well known that the catalytic properties of a bimetallic catalyst depend upon its surface composition.[1,2] Many material properties and metallurgical phenomena can be understood from the segregation of one species to an interface or to the surface.[3,4] Although several sophisticated surface analytical tools have been used to study surface segregation, accurate equilibrium in-depth composition profiles with atomic layer depth resolution have been obtained only by the time-of-flight atom-probe field ion microscope (AP-FIM).[5,6]

Earlier investigations of Ni–Cu and Pt–Au alloys have found that Cu strongly segregates to the top layer with a slight Cu depletion from the second to the fifth layer,[5] and Au segregates to the top four layers of the surface.[6] This work has been initiated to obtain detailed information on the nature of compositional variation in near surface layers in binary alloys, particularly the Pt base alloys which are important in catalysis.[7] Equilibrium concentration depth profiles with single atomic layer depth resolution have been obtained for five different Pt–Rh alloys and one Pt–Ir alloy on the (001) plane.[8,9] Along with the segregation of alloy constituents, a minute amount of impurity sulfur in the bulk has been found to cosegregate to the surface and to form an overlayer on the surface. Sulfur has a strong poisoning effect in many catalytic reactions,[10] therefore a study of the effect of sulfur on the compositional features of alloy surfaces is very important.

A brief description of the experimental procedure will be presented in Sec. II. The alloy surface segregation results along with the effect of cosegregated sulfur and the structure of sulfur overlayer are discussed in Sec. III. A brief summary of recent results obtained by the atom-probe and a general discussion of the atom-probe equilibrium in-depth concentration profiles data on the understanding of atomic interactions in the surface region is presented in Sec. IV.

II. EXPERIMENTAL PROCEDURE

Experimental procedure for obtaining surface segregation results using an atom probe[11] has been outlined in previous reports.[5,6,8,9] A very brief description of the experiment and the specific features observed in the alloys in this study will be presented here.

A. Sample preparation

The alloy samples used in this study are made from 0.004 in. diameter wires. The wires are first annealed by resistive heating in a vacuum station in 10^{-9} Torr pressure. The annealing is continued for several days at a temperature higher than 700 to 900 °C to clean the samples of impurities and to enlarge the grains in the crystals. The alloy samples are made in the form of sharp needles by electrochemical polishing and mounted on molybdenum heating loops. After a tip is put inside the chamber, procedure for obtaining ultrahigh vacuum is followed. The ultimate vacuum routinely obtained during this investigation is 2×10^{-10} Torr or better. The alloy tips are annealed in the microscope chamber for a long period of time to further clean the samples. The tips are then field evaporated to a nearly hemispherical, atomically perfect surface.

B. Bulk composition

A mass spectrum of several thousand atoms is obtained by slow field evaporation, about an ion detected per 20 pulses, for bulk compositional analysis of the alloy. The pulse voltage is always set at approximately 20% of the total voltage. This eliminates the problem of possible preferential

 0021-9606/85/130388-09$02.10

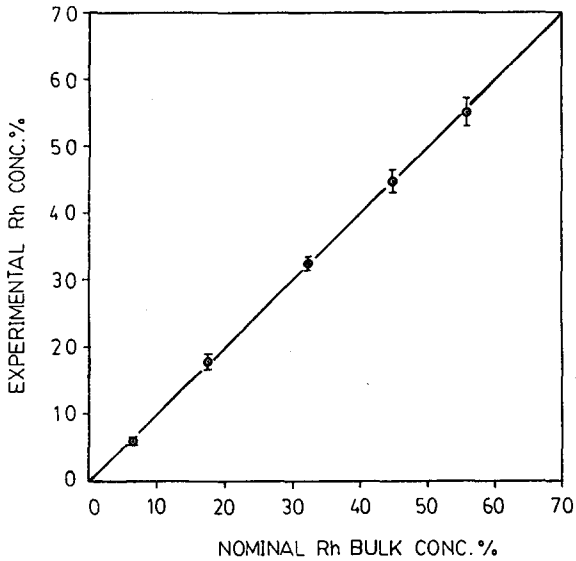

FIG. 1. Comparison between the nominal bulk composition and the bulk composition determined by the atom probe for the five Pt–Rh alloys studied. The pulse-voltage fraction used is approximately 20% of the total voltage.

dc field evaporation of one species which may result in incorrect bulk compositional determination. Figure 1 shows a plot of the nominal composition or the composition supplied by the manufacturer, and the experimentally determined bulk composition of several Pt–Rh alloys used in this study. The agreement suggests that using 20% of the total voltage as the pulse voltage should eliminate the problem of preferential dc field evaporation. Such condition has always been maintained during the course of this study. Furthermore, no impurity atom has been found in more than ten thousand atoms detected from the bulk of the samples. Therefore the impurity level is less than 100 ppm, as was also claimed by the manufacturer.

C. Surface segregation study

1. Annealed endform

Once a well developed nearly hemispherical tip surface has been obtained by dc field evaporation and the crystallographic planes identified as seen on the field ion (FI) image, the tip is annealed at 700 °C for 5 min in field free condition in a vacuum of 2×10^{-10} Torr or better. This allows the redistribution of the alloy species in the sample. The tip is then quenched to $\sim$78 K at a rate of $\sim10^4$ K/s which practically freezes the alloy species distribution equilibrated at 700 °C. The tip is then imaged again by cautiously raising the dc field. After each annealing the central (001) plane develops into a large facet as observed in the FI image. It has been observed earlier that sometimes an FI image shows an extremely dim image of the top layer in some alloy systems such as Ni–Cu due to strong segregation of one of the species.[5] For all the alloys investigated in this study, a somewhat different phenomenon has been observed.

As the dc field is gradually raised (still below the evaporation field) the FI image of the thermal endform shows several spots close to the edge of the top layer. On further raising

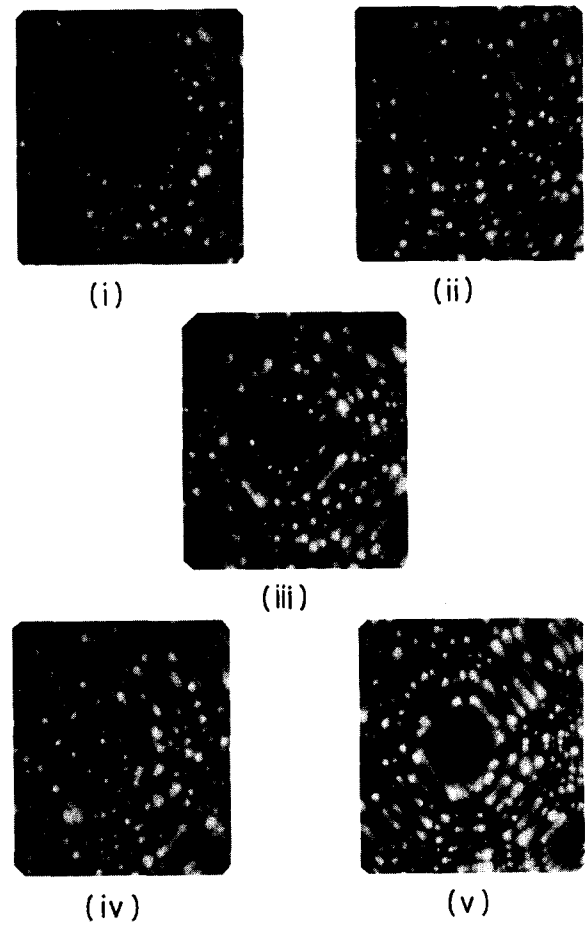

FIG. 2. Field ion images of the (001) plane of a Pt–21.3 at. % Ir sample annealed at 700 °C for 5 min. The overlayer and the first layer field evaporate and shrink in size together as shown from (i) to (iv). After these two layers are field evaporated, the image appears normal, and an FIM image of the second layer is shown in (v).

the field these spots become brighter and form the edge of an overlayer. These atoms are found to be more resistive to field evaporation compared to the alloy constituents and they evaporate together with the edge atoms of the substrate layer. Due to the problem of field evaporating the overlayer smoothly or resolving the edges of the overlayer and the first layer, these two edges are considered as one and field evaporated together. No such impurities have been found beyond the first layer. Figure 2 shows the FI image of the (001) plane and the subsequent field evaporation sequence of the first layer and the overlayer for a Pt–21.3 at. % Ir alloy annealed at 700 °C.

2. Aiming procedure

Once the thermal endform is obtained, the tip position is adjusted so that the edge of the top layer (in this case both the edges of the top layer and the overlayer) is aimed at the probe hole. The channel plate screen assembly is flipped out of the way and a slow pulse field evaporation is continued. Atoms evaporate as charged ions from the plane edge and only those covered by the projected probe hole area go through it and are subsequently detected. This causes the layer to shrink (in this case both the overlayer and the top layer shrink together) and the tip position is readjusted to align the edge(s) of the

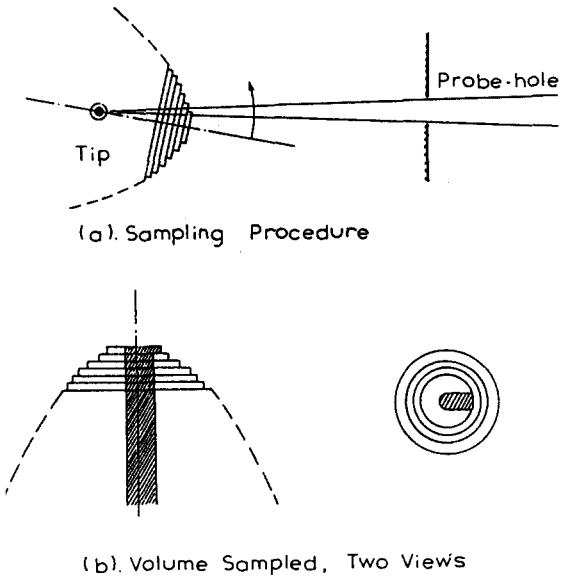

FIG. 3. The sampling method used in this study for atomic layer by atomic layer compositional analysis. (a) Field evaporation proceeds from plane edges, thus the probe hole is aimed at the plane edge. As the top layer reduces in size, the probe hole is adjusted accordingly. (b) Volume of the specimen analyzed using this sampling method. Note that only the edge effect of the first layer can be detected.

top layer with the probe hole. This aiming procedure is illustrated in Fig. 3. Similar pulse evaporation is continued and ions from the edge(s) are detected. The process is continued until the entire top layer(s) is removed and then repeated for subsequent layers in the same manner. The signals detected from each layer separately constitute one set of concentration depth profile (CDP) data. The sequence of detected signals from the plane edge to the plane center constitutes one set of lateral concentration profile (LCP) data. The volume sampled is also shown in Fig. 3.

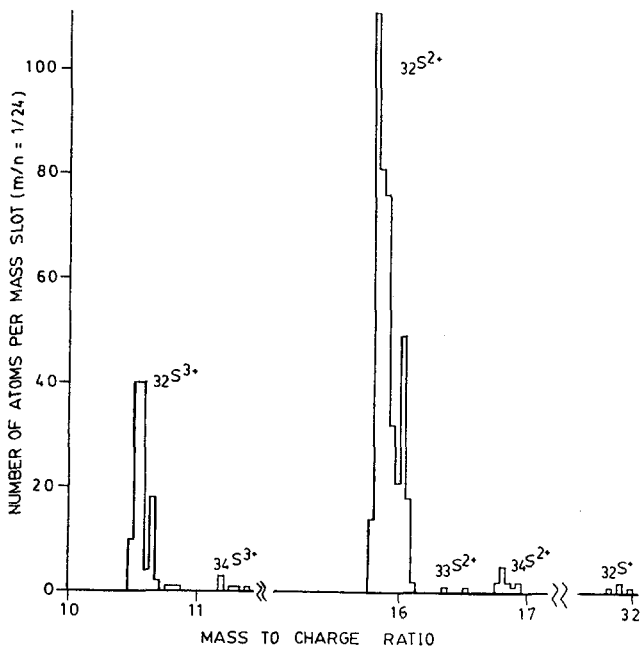

FIG. 4. Histogram of the combined mass spectrum of sulfur detected from the annealed surfaces of the five Pt–Rh alloys. The mass-to-charge ratios of all the mass lines are shifted by ~1% to the low side since our calibration constant was off by ~1% the correct value. We present the data as appear in the computer printout.

TABLE I. Isotopic abundances of sulfur.

Isotope	Detected number of ions	% Abundance (experimental)	% Abundance[a] standard
^{32}S	796	95.8 ± 0.7	95
^{33}S	6	0.7 ± 0.3	0.8
^{34}S	29	3.5 ± 0.6	4.2

[a]From Ref. 12.

As this is a single ion detection process, the amount of data obtained is inherently small, usually between 25 to 80 ions from each layer. To obtain a statistically reliable amount of data, the experiment is repeated several times for several tips under identical heat treatment, and the accumulated data is reported with the respective statistical uncertainty. The statistical uncertainty in composition is calculated using the following relation:

$$\delta(\%) = \frac{100\%}{N_A + N_B}\left(\frac{N_A N_B}{N_A + N_B}\right)^{1/2}, \tag{2.1}$$

where N_A and N_B represent, respectively, the number of A and B atoms detected within a layer. The number of ions detected from each layer ranges between several hundred to more than a thousand ions for these alloys as reported in earlier papers.[8,9]

The nature of field evaporation and the visual aid of aiming contribute to the unique feature of this result as having a true single atomic layer depth resolution. Although intermixing of signals from the overlayer and the top layer has occurred, it does not affect the depth resolution since in this special case the top layer composition is easily derived by subtracting the impurity signals of the overlayer. With the procedure we have followed, we are able to determine the overlayer coverage, and the effect of the overlayer on the segregation behavior of the alloy. These will be discussed in the next section.

III. RESULTS AND DISCUSSION

A. Impurity segregation and overlayer formation

A minute amount of impurities in the alloy will segregate to the surface and form an overlayer. Most of the ions detected from the overlayer have a mass to charge ratio of 16 amu indicating that these atoms are either chemisorbed oxygen from the background vacuum or cosegregated impurity sulfur from the bulk. The RGA mass spectrum shows no detectable oxygen peak in the 10^{-10} Torr range. A plot of the combined histogram of the mass signals from the overlayer as detected from the five Pt–Rh alloys is shown in Fig. 4. The mass peaks indicate that these atoms are impurity sulfur atoms segregated to the surface. A further evidence is the excellent agreement between the isotopic abundances of these overlayer atoms presented in Table I with the standard table values[12] of sulfur which are also listed in the table. For

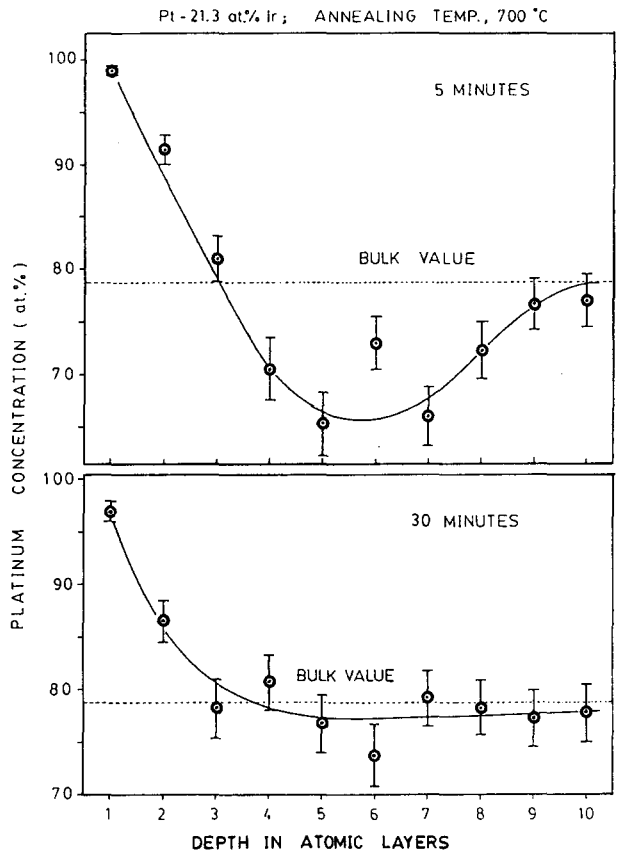

FIG. 5. Composition depth profiles of the (001) plane of a Pt–21.3 at. % Ir alloy with 5 and 30 min annealing at 700 °C. The 5 min data shows an iridium rich region from the fourth to the eighth layer. This feature is due to a diffusion kinetic limited effect discussed in the text.

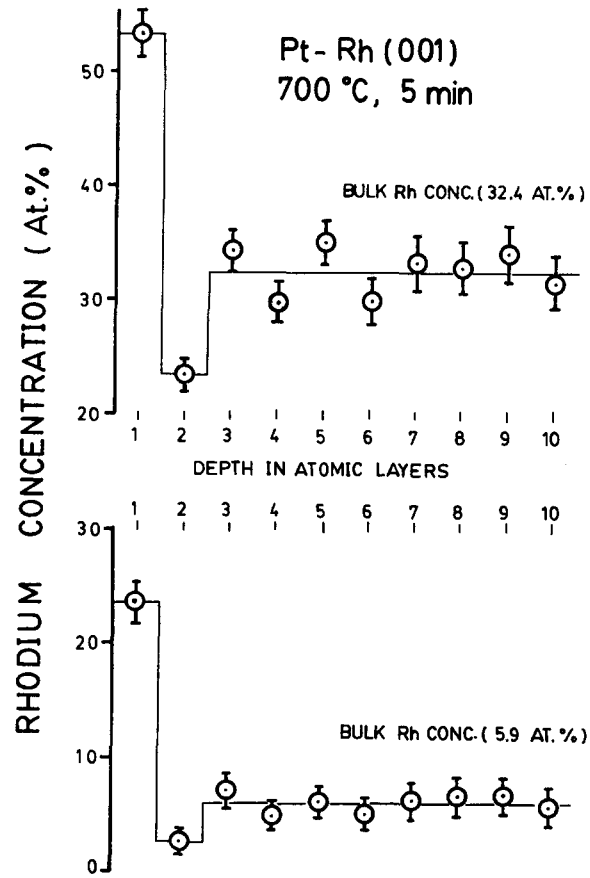

FIG. 6. Composition depth profiles of a Pt–32.4 at. % Rh and a Pt–5.9 at. % Rh alloy (001) plane obtained after annealing the samples at 700 °C for 5 min.

one alloy, the Pt–32.4 at. % Rh alloy (from a different company), a small amount of arsenic is also detected. Thus the minute amount of impurity sulfur in the bulk segregates to the surface and forms an overlayer on the (001) plane of Pt–Rh and Pt–Ir alloys.

B. Surface segregation of alloy constituents

Two concentration depth profiles (CDPs) for the (001) plane of a Pt–21.3 at. % Ir alloy are shown in Fig. 5. One of the CDPs is obtained by annealing the sample at 700 °C for 5 min and the other is obtained by annealing at 700 °C for 30 min. Both these profiles show Pt enrichment on the top two layers. The 30 min data indicates a monotonic decrease of Pt concentration into the bulk while the 5 min data shows a nonmonotonic decrease into the deeper layers. The latter case is where the sample has not reached global thermodynamic equilibrium with an annealing period of 5 min, and this point will be further discussed later.

Figure 6 shows two CDPs for the (001) plane of two different Pt–Rh alloys annealed at 700 °C for 5 min. Both these alloys show Rh segregation to the first layer with a significant Rh depletion in the second layer. The alloy composition returns to the bulk value from the third layer on. Three more alloys of different Rh bulk concentration have been studied and all of these show similar behavior. Figure 7 shows the Rh concentration in the first three layers plotted against the bulk concentration. All these CDPs are in ther-

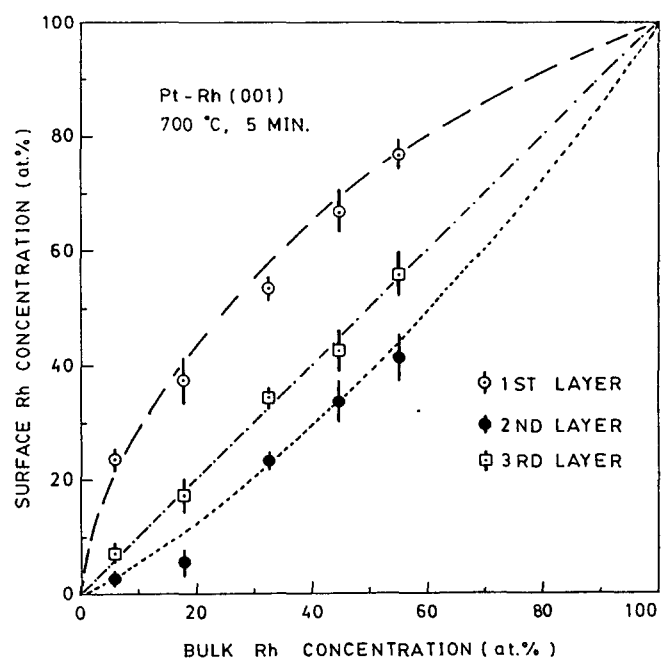

FIG. 7. Rh concentration in the top three surface layers for the (001) plane plotted against the bulk Rh concentration in five Pt–Rh alloys. Data are obtained by annealing the samples at 700 °C for 5 min.

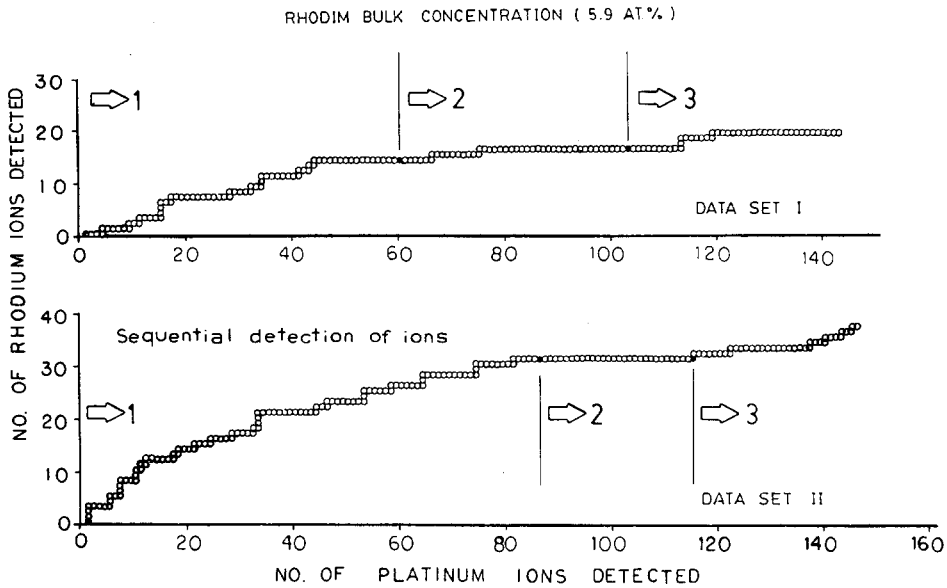

FIG. 8. Lateral concentration profiles of a Pt–5.9 at. % Rh alloy (001) plane at 700 °C. The arrow indicates lateral direction from the edge to the center of the numbered layer, i.e., the first, second and third layer.

modynamic equilibrium and is verified by annealing one sample at a higher temperature and obtaining a statistically reliable CDP. This will be discussed shortly.

The sequential detection process is demonstrated in lateral concentration profiles (LCPs) of a Pt–5.9 at. % Rh alloy–as shown in Fig. 8. Sequential plots of this nature have been routinely used for bulk compositional analysis of refractory metal–silicide using atom-probe data.[13] In the present case, if a significant concentration variation exists within a plane, i.e., from the edge to the center, the profiles would show a consistent repetition of the variation beyond the inherent statistical fluctuation of such detection process. The two LCPs indicate within expected statistical uncertainties a uniform Rh surface concentration in the plane. In addition these LCPs do not show any edge effect which may be expected in such experiments. The degree of surface enrichment of one species increases with decreasing coordination number of a site. Thus the degree of enrichment is of the following order, e.g., kink > edge > plane. The samples used are nearly hemispherical tips and have flat planes and highly stepped surfaces. As indicated in Fig. 3, the edge of the top layer is the only edge which is sampled in our experiment. The spatial extent of the edge effect is limited to only a few atomic dimensions, and the number of atoms detected from the edge of the thermal endform is rather small. Thus unless the effect is very strong, it will not be easy to detect. Furthermore, the presence of the impurity overlayer makes it difficult to aim at the edge with the desirable precision. All these profiles presented here do not account for the overlayer coverage and its interaction with the substrate. This is discussed in the following section.

C. Overlayer–substrate interaction

Figure 9 shows two LCPs for the impurity sulfur concentration of a Pt–5.9 at. % Rh alloy. These profiles show a uniform coverage of impurity on the top layer. All such LCPs are plotted as a routine check and it is found to be consistent from one set of data to another. Sulfur concentra-

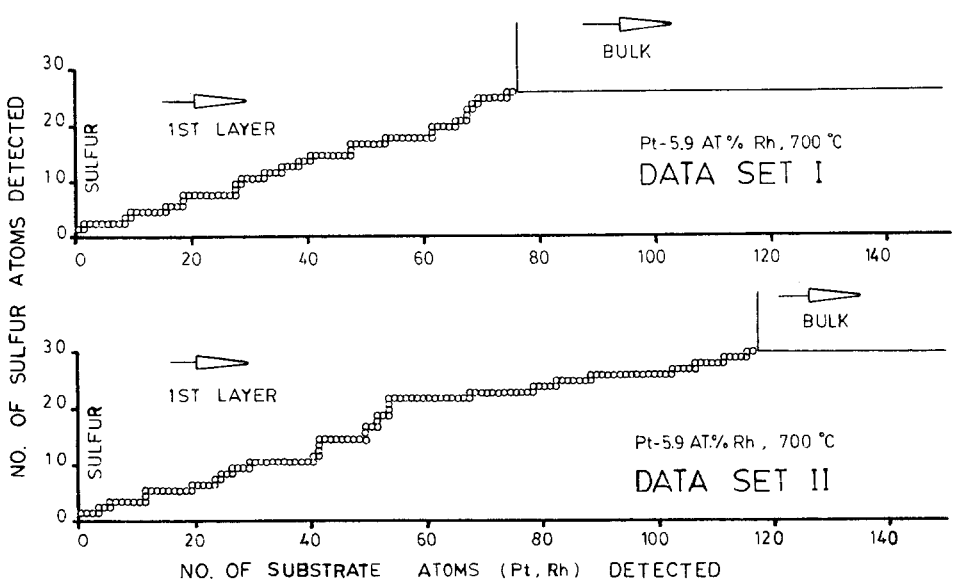

FIG. 9. LCPs of cosegregated sulfur on the surface of a Pt–5.9 at. % Rh alloy (001) plane. The sample was annealed at 700 °C.

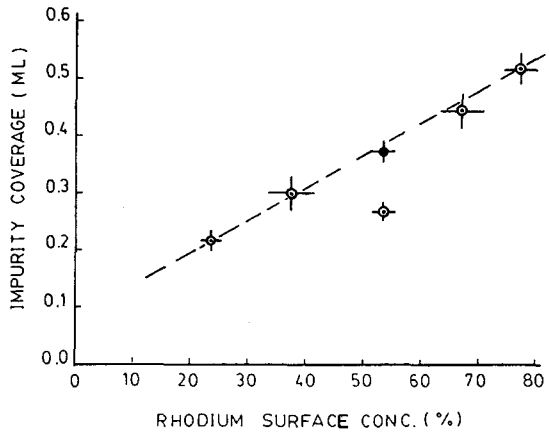

FIG. 10. A plot of the dependence of the impurity coverage on surface Rh concentration for Pt–Rh (001) plane at 700 °C. Open circles represent sulfur coverage only and the closed circle represents combined sulfur and arsenic coverage.

tion beneath the first layer is practically zero, although occasionally one or two sulfur atoms are detected. The Rh surface concentration on the first layer of the (001) plane and the corresponding sulfur coverage for all five Pt–Rh alloys are plotted in Fig. 10. It shows that sulfur coverage ranges between 0.22 to 0.52 monolayer and this coverage increases with increasing Rh surface concentration or with decreasing Pt surface concentration. This indicates that Rh–S chemisorption bond formation may be energetically more favorable than the Pt–S bond. For the Pt–Ir (001) plane, ~0.18 monolayer coverage has been found, indicating that Pt–S bond may be stronger than Ir–S bond. However, with only one Pt–Ir alloy studied, this conclusion is only tentative.

Although in principle one can study the formation of these bonds by treating the field evaporation events as a Markov chain,[14] we are not able to do it here since the sulfur atoms are not in the same layer as the metal atoms. Their field evaporation behavior is not well understood either.

D. Overlayer structure

Field ion microscope is capable of obtaining a direct image of an overlayer superstructure if the overlayer can withstand the applied high field and if the overlayer does not cause any rearrangement of substrate geometry. One such example is silicon superstructure on W(110) as observed by Tsong and Casanova.[15] A high resolution FIM with a Displex refrigerator has been used to investigate the overlayer structure. Although the 15 K images obtained by this FIM do not convincingly establish any superstructure, nevertheless it provides some indication of ordering of the overlayer atoms. Figure 11 shows the FI image of a Pt–5.9 at. % Rh alloy annealed at 700 °C. A possible resemblance of the overlayer structure as imagined from the rows of individual image spots is a $c(2\times2)$ superstructure also shown in Fig. 11. It is seen that the edge of the first layer is not as clear except for a few atoms imaged outside the square matrix. This indicates that the sulfur atoms tend to resist field evaporation. It is not clear however, why the sulfur atoms inside the square matrix do not image as bright spots. The difficulty in imaging smaller atoms in a host matrix has always been a problem to field ion microscopy.[16] The conclusion is that the detailed imaging properties of sulfur have to be understood before any accurate determination of such overlayer structure can be made. Even though adsorbed sulfur superstructure on Pt surfaces is well established from LEED studies,[17,18] it may not be correct to predict the same ordering for the alloy surface, especially since the sulfur coverage is found to be related to Rh concentration. Since the experimental data indicates a slightly stronger attractive interaction bond between Rh and S than between Pt and S, it may then be appropriate to expect that for a random distribution of Rh on the surface the structure of sulfur overlayer may tend to be also disordered. This is an interesting problem which has to be further investigated.

E. Segregation kinetics

1. Pt–Ir system

The nonmonotonic nature of the CDP for the Pt–Ir alloy with 5 min annealing time as shown in Fig. 5 can be explained to be a diffusion kinetic limited effect. During an annealing period the alloy constituents have to exchange po-

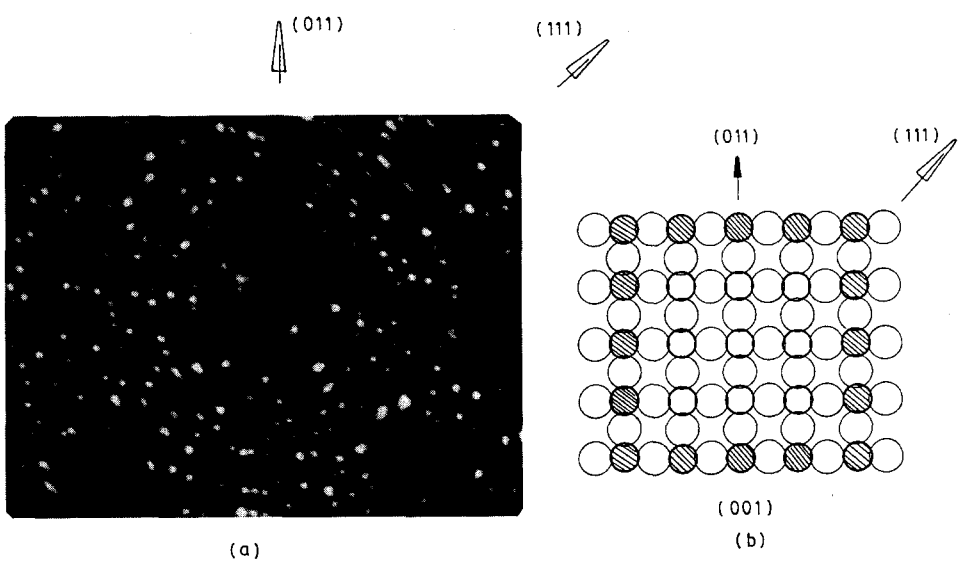

FIG. 11. (a) FI image of an overlayer formed on the (001) plane of a Pt–5.9 at. % Rh sample after annealing at 700 °C for 5 min. A few atoms in the first layer are seen also. (b) A $c(2\times2)$ overlayer structure corresponding to the observed overlayer structure. Edge atoms of the overlayer are shaded to show a resemblance to the FI image shown in (a).

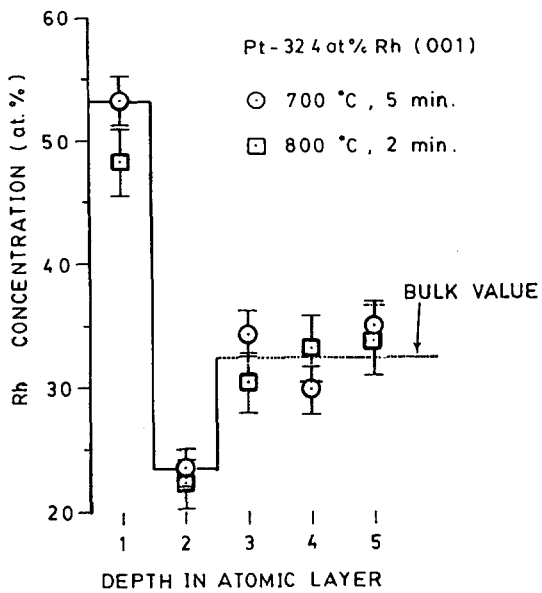

FIG. 12. CDPs for the first five layers of a Pt–32.4 at. % Rh (001) plane obtained after 5 min annealing at 700 °C (circles) and after 2 min annealing at 800 °C (squares).

sitions and diffuse through the bulk to achieve thermodynamic equilibrium. And this is achieved if the diffusion lengths for both the alloying species are sufficiently large. Unfortunately no tracer diffusion data is available for Pt–Ir in the literature to make a proper estimation of the diffusion lengths. A close approximation is to use the self-diffusion data. For Pt, the activation energy for self-diffusion is 2.96 eV with a preexponential factor of 0.33 cm^2/s.[19] With these values the self-diffusion coefficient of Pt is

$$D = 0.33 \exp(-2.96\text{eV}/kT)\ \text{cm}^2/\text{s}. \tag{3.2}$$

It can be shown that the diffusion length ($\sqrt{6Dt}$) of Pt for 5 min annealing at 700 °C is ~52 Å and that for 30 min annealing is ~129 Å. Both these values are quite sufficient to ensure thermodynamic equilibrium. Similar surface enrichment of Pt for both cases is a proof of this. Furthermore, it is known that thermodynamic equilibrium is achieved via grain boundary diffusion and surface diffusion as well as bulk diffusion, and equilibrium can be achieved much faster by a combination of all three diffusion mechanisms. Moreover, the tip geometry, which presents a much higher surface to volume ratio than a planar surface, should achieve global equilibrium even faster than in planar geometry.

Hofmann and Erlewein developed a kinetic model in which the time evolution of solute surface enrichment is used to calculate diffusivities of the solute in the alloy.[20] The present case is slightly different since both the 5 and the 30 min annealing achieve a similar surface enrichment of Pt. As Pt segregates to the surface, the displaced Ir atoms move into the bulk and the 5 min annealing profile shows an accumulation of these Ir atoms in deeper layers. The average diffusion length, as determined from the distance between the surface and the peak of the diffusion front is approximately four atomic layers or ~8 Å. It can also be noted that the average diffusion length of the Ir atoms is approximately the same as the width of the diffusion front. The diffusivity can be estimated from

$$(r)_{\text{rms}} = \sqrt{6Dt}, \tag{3.3}$$

where $(r)_{\text{rms}} \simeq 8$ Å, $t = 300$ s. With these values, the diffusion coefficient of Ir in Pt–21.3 at. % Ir at 700 °C is

$$D \simeq 3.55 \times 10^{-18}\ \text{cm}^2/\text{s}. \tag{3.4}$$

Using an equation similar to Eq. (3.2) and the same preexponential factor, the activation energy Q is found to be ~3.3 eV. With this diffusivity, the diffusion length of Ir for a 30 min annealing period is ~20 Å, i.e., 10 atomic layers. The 30 min annealing profile is consistent with it, since the Ir rich layers have disappeared. As time progresses the diffusion front should also disperse. It is impractical to make a time-temperature study of diffusion using this technique due to the time consuming nature of this experiment. The calculated value of the Ir diffusivity is an approximate value and should be accurate within an order of magnitude.

2. Pt–Rh system

To establish whether the Rh depletion in the second layer is a transient distribution or an equilibrium distribution, one alloy Pt–32.4 at. % Rh is annealed at 800 °C for 2 min and a statistically reliable set of data is obtained for the first five layers of the (001) plane. This set of data together with that of 700 °C annealing for 5 min are shown in Fig. 12. Both these data show similar nonmonotonic composition variation.

No self-diffusion data on Rh is available to make an estimate of Rh diffusivity length. However the self-diffusion coefficient of Rh in Rh may be estimated from the van-Liemp relation, which is approximately correct for most metals. The relation states that the activation energy of self-diffusion (Q) is related to the melting point by $Q = 34\,T_m$ (K). Hence for Rh ($T_m = 2239$ K) the value of Q is 76.13 kcal/mol or 3.3 eV. Assuming the same preexponential factor as for Pt, then

TABLE II. Comparison of the diffusivities and the diffusion lengths for self-diffusion of Pt and Rh for different temperatures and for different annealing periods.

Element	Activation energy Q (eV)	700 °C Diffusivity cm^2/s	700 °C $(r)^{5\text{ min}}_{\text{rms}}$ Å	800 °C Diffusivity cm^2/s	800 °C $(r)^{2\text{ min}}_{\text{rms}}$ Å
Pt	2.96	1.56×10^{-16}	52	4.20×10^{-15}	173
Rh	3.30	2.70×10^{-18}	7	1.06×10^{-16}	28

TABLE III. Binary alloy surface segregation behavior observed in atom-probe studies.

Alloy sytem	Segregating element	Extent of segregation (no. of atomic layers)	Nature of convergence to bulk value	Reference
Pt–Rh	Rh	1	oscillatory	9
Pt–Ir	Pt	2	monotonic	8
Pt–Au	Au	4	monotonic	6
Ni–Cu	Cu	1	oscillatory	5

$$D = 0.33 \exp(-3.3\ \text{eV}/kT)\text{cm}^2/\text{s}. \quad (3.5)$$

Table II lists the diffusivities and the appropriate diffusion lengths for Pt and Rh for the two different annealing periods. It is evident that if Rh depletion in the second layer were a transient effect, the annealing involving four times longer diffusion length should have removed such a depleted region. The estimate given for Rh is a worst case estimate, and still Rh depletion is observed. Thus we believe the nonmonotonic concentration profiles observed for Rh are true thermodynamic equilibrium profiles.

It can also be noted that the surface Rh concentration at 800 °C is slightly lower than that at 700 °C. This is consistent with segregation theories.[21,22]

F. Discussion

Segregation of Pt in Pt–Ir alloy is consistent with all the existing theoretical models. The interesting feature is the monotonic decrease of Pt concentration into the bulk value instead of an abrupt change. Such a feature has previously been observed for Pt–Au alloys where Au segregates to the top four layers.[6]

Segregation of Rh to the surface of Pt–Rh alloy is consistent with the bond-breaking model since Rh has the lower heat of sublimation. According to the atomic model proposed by Abraham *et al.*,[23] the size ratio of rhodium (solute) to platinum (solvent) is $\sigma^* = 0.969$,[24] and the bond strength ratio is $\epsilon^* = 0.969$.[25] These values support Rh segregation as indicated by the universal segregation map proposed in their paper. However according to a later modification of this model by Abraham,[26] the surface energy ratio $\gamma^* = 1.032$ and $\sigma^* = 0.969$ lies inside the universal curve proposed for solute segregation and thus Rh should not segregate. The surface energy theory of Hamilton,[27] and the simplified electronic model of Lambin *et al.*[28] predict Pt segregation. Experimentally, Williams and Nelson reported observation of Pt segregation in Pt–Rh alloys in an ion scattering experiment.[29] Unfortunately no details of their experimental condition such as vacuum and impurity level and details of results were given in their paper which is a summary abstract.

The disagreement between various models is not uncommon. However it is difficult to say with any certainty which model is correct for this system due to the presence of an adsorbed sulfur layer. Our observation of Rh enrichment may indicate a chemisorption effect. It is likely that if the Rh–S bond is stronger than the Pt–S bond, then the chemisorption induced segregation will become predominant.[30] Unfortunately no theoretical work is available for unequivocal interpretation of our data. Obviously, our next project should study surface segregation of high purity Pt–Ir and Pt–Rh alloys, so that this question can be resolved by experiment.

The most interesting finding for these alloys is the depletion of Rh in the second layer. We have carefully established that these nonmonotonic composition depth profiles are real and are thermodynamic equilibrium profiles. Such profiles have only been treated by quasichemical calculations.[31,32] The basic assumption is the bond relaxation at the surface. In an appropriate way the amount of such relaxation is estimated which shows that an oscillatory profile can result. A recent Monte Carlo calculation by King and Donnelly has also found such oscillatory nature in some alloys by using the surface modified pair potential.[33]

A recent pseudopotential calculation by Barnett *et al.* shows that a single ion potential at simple metal surfaces oscillates around a bulk value and decays within a few atomic layers.[34] It is this oscillation that determines the equilibrium structure of the surface and any surface relaxation. It may be possible that the single ion potential is also responsible for the oscillatory composition profile, since the segregating elements should redistribute under the influence of such a potential.

The recent results obtained by the atom probe for several alloy systems are listed in Table III. It is found that the compositional variation in the near surface region can be both monotonic and nonmonotonic in nature, and the enrichment of segregants can extend to one to a few atomic layers in depth depending on the alloy system.

IV. SUMMARY AND CONCLUSION

Surface segregation behavior of a Pt–Ir and five Pt–Rh alloys has been studied with a time-of-flight atom probe. It is found that a very minute amount of impurity sulfur in the bulk of these alloys can segregate to the surface and form an overlayer. In addition, Pt segregates to the top two layers on the (001) plane of the Pt–Ir alloy, and Rh segregates only to the top layer on the (001) plane of the Pt–Rh alloys. The sulfur coverage on the Pt–Rh surface ranges between 0.22 to 0.52 monolayer and increases with increasing Rh surface concentration. This correlation strongly suggests an attractive interaction between Rh and S atoms.

It is shown that diffusion effects in surface segregation of alloys can be studied with the atom probe. However, the time consuming nature of the experiment makes such a measurement impractical. The segregation behavior of these alloys can be interpreted with existing theoretical models. The cosegregation of both Rh and S in Pt–Rh alloys may represent a chemisorption induced surface segregation phenomenon.

As the atom probe can provide accurate information on the compositional variation in the near surface layers of alloys with a single atomic layer depth resolution, these data should be useful to both theorists and experimentalists. The agreement or disagreement between theories and experiments regarding whether a particular species segregates to the surface or not is interesting. Such information would lead to a better qualitative understanding of surface segregation, and there are several macroscopic techniques better suited for this purpose. The quantitative data obtained by the atom probe are, however, better suited for understanding atomic interactions in the near surface layers of a solid. The wide variety of compositional variations in the near surface layers we have obtained with the atom probe should shed some light on these interactions. Surface relaxation and reconstruction processes are of considerable interest and the compositional depth profiles strongly indicate one or both of these processes may be responsible for giving rise to the different compositional variations in the surface layers we have observed.

ACKNOWLEDGMENTS

The work was supported by the NSF under grant number DMR-8217119. The authors also acknowledge the valuable technical assistance of S. B. McLane.

[1]V. Ponec, Surf. Sci. **80**, 352 (1979).
[2]W. M. H. Sachtler and R. A. Van Santen, Appl. Surf. Sci. **3**, 121 (1979).
[3]D. McLean, *Grain Boundaries in Metals* (Oxford University, Oxford, 1957).
[4]C. J. McMahan, Jr. and L. Marchut, J. Vac. Sci. Technol. **15**, 450 (1978).
[5]Y. S. Ng, T. T. Tsong, and S. B. McLane, Jr., Phys. Rev. Lett. **42**, 588 (1979).
[6]T. T. Tsong, Y. S. Ng, and S. B. McLane, Jr., J. Chem. Phys. **73**, 1464 (1980).
[7]J. C. Rasser, *Platinum–Iridium Reforming Catalysts* (Delft University, Delft, The Netherlands, 1977).
[8]M. Ahmad and T. T. Tsong, Appl. Phys. Lett. **44**, 40 (1984).
[9]M. Ahmad and T. T. Tsong, Surf. Sci. **149**, L7 (1985).
[10]J. Oudar, Catal. Rev. Sci. Eng. **22**, 171 (1980).
[11]E. W. Müller and T. T. Tsong, *Field Ion Microscopy, Principles and Applications* (Elsevier, New York, 1969).
[12]*Handbook of Chemistry and Physics*, 55th ed., edited by R. C. Weast (CRC, Cleveland, 1974–1975).
[13]T. T. Tsong, S. C. Wang, H. F. Liu, H. Cheng, and M. Ahmad, J. Vac. Sci. Technol. B **1**, 915 (1983).
[14]T. T. Tsong, S. B. McLane, Jr., M. Ahmad, and C. S. Wu, J. Appl. Phys. **53**, 4180 (1982).
[15]T. T. Tsong and R. Casanova, Phys. Rev. Lett. **47**, 113 (1981).
[16]T. T. Tsong and E. W. Müller, Appl. Phys. Lett. **9**, 7 (1966).
[17]W. Heegeman, K. H. Meister, E. Bechtold, and K. Hayek, Surf. Sci. **49**, 161 (1975).
[18]R. J. Madix, S. B. Lee, and M. Thornburg, J. Vac. Sci. Technol. A **1**, 1254 (1983).
[19]N. L. Peterson, J. Nucl. Mater. **69**, 1 (1978).
[20]S. Hofmann and J. Erlewein, Surf. Sci. **77**, 591 (1978).
[21]G. Kerker, J. L. Moran-Lopez, and K. H. Bennemann, Phys. Rev. B **15**, 638 (1977).
[22]S. Mukherjee, J. L. Moran-Lopez, V. Kumar, and K. H. Bennemann, Phys. Rev. B **25**, 730 (1982).
[23]F. F. Abraham, N.-H. Tsai, and G. M. Pound, Surf. Sci. **83**, 406 (1979).
[24]*Metal Handbook* (ASM, Metal Park, Ohio, 1961), Vol. 1.
[25]*American Institute of Physics Handbook* (McGraw–Hill, New York, 1957).
[26]F. F. Abraham, Phys. Rev. Lett. **46**, 546 (1981).
[27]J. C. Hamilton, Phys. Rev. Lett. **42**, 989 (1979).
[28]Ph. Lambin and J. P. Gaspard, J. Phys. F **10**, 2413 (1980).
[29]F. L. Williams and G. C. Nelson, J. Vac. Sci. Technol. **16**, 663 (1979).
[30]D. Tomanek, S. Mukherjee, V. Kumar, and K. H. Bennemann, Surf. Sci. **114**, 11 (1982).
[31]Y. S. Ng, T. T. Tsong, and S. B. McLane, Jr., Surf. Sci. **84**, 31 (1979).
[32]V. Kumar, Phys. Rev. B **23**, 3756 (1981).
[33]T. S. King and R. G. Donnelly, Surf. Sci. **141**, 417 (1984).
[34]R. N. Barnett, R. G. Barrera, C. L. Cleveland, and U. Landman, Phys. Rev. B **28**, 1667 (1983); R. N. Barnett, U. Landman, and C. L. Cleveland, *ibid.* **28**, 6647 (1983).